D25

N79-24026

# MAGNETIC SHIELDING OF LARGE HIGH-POWER-SATELLITE SOLAR ARRAYS USING INTERNAL CURRENTS

Lee W. Parker
Lee W. Parker, Inc.

William A. Oran
NASA Marshall Space Flight Center

## SUMMARY

Present concepts for solar power satellites involve dimensions up to tens of kilometers and operating internal currents up to hundreds of kiloamperes. The question addressed here is whether the local magnetic fields generated by these strong currents during normal operation (effectively providing the array with its own "magnetosphere") can shield the array against impacts by plasma ions and electrons (and from thruster plasmas) which can cause possible losses such as power leakage and surface erosion. An affirmative answer is indicated by approximate solution of the inherently 3-D problem.

In the present work one of several prototype concepts has been modeled by a long narrow rectangular panel 2 km wide and 20 km long. The currents flow in parallel across the narrow dimension (sheet current) and along the edges (wire currents). The wire currents accumulate from zero to 100 kiloamp and are the dominant sources. The magnetic field is approximated analytically as due to separate sheet and locally constant wire currents. The equations of motion for charged particles in this magnetic field are analyzed using conservation of canonical momentum to find dynamical limits of the motion, that is, regions inaccessible to the particles. The ion and electron fluxes at points on the surface are represented analytically for monoenergetic distributions and are evaluated by Parker's quadrature technique for Maxwellian particle velocity distributions. Sample numerical results for electrons and protons correlate well with the ratios of (a) the particle gyroradius to the array width and (b) the particle momentum to the critical momentum $e\mu I$, where e is the particle charge, $\mu$ is the magnetic permeability, and I is the wire current. The field will prevent kilovolt protons and mev electrons from reaching significant fractions of the surface.

The analysis is applicable to both low earth orbit and geosynchronous orbit, when appropriate particle masses and temperatures are substituted. It suggests that the current distribution may be designed so as to optimize the shielding and that the solar cell lifetime in orbit may be prolonged by a possible factor of 5.

## INTRODUCTION

For the purposes of the present analysis of magnetic shielding, we assume a model suggested by a Rockwell International study (ref. 1 and fig. 1). It is represented in the simplified manner shown in figure 2. Here we have a flat panel, lying in the x-y plane, made up of strips of photovoltaic cells. Each strip is of length 2X and consists of photovoltaic cells connected in series along the x-direction. The strips of cells are stacked in the y-direction and are electrically connected in parallel at their ends to end-bus wires at positions x = +X and x = -X. The array extends from y=0 to y=L. Electric fields are neglected, which should be valid for thin sheaths.

This arrangement yields a current-flow distribution as follows. The cross-current flows from bus to bus in the +x direction, and the currents accumulate along the bus wires. Therefore, we have essentially two kinds of currents as sources for magnetic fields:

(1) a surface current density (a "sheet current") in the plane of the panel, directed in the +x direction, with the current per unit length (K) independent of x and y, and

(2) a "wire current" (I) due to flow in the bus wires, directed in the +y and -y directions, which accumulates from zero amps at y=0 to $10^5$ amps at y=L. The variation can be assumed to be linear in y, although this assumption is not essential.

For the purpose of calculating magnetic fields, these assumptions allow us to establish the current sources as K=5 amp/meter and $I=I_0 \cdot (y/L)$ amp, where L is 20 km in figure 2 and $I_0$ is $10^5$ amp. We assume further that, except near the ends of the array, the magnetic field in the vicinity of the array is the superposition of two contributions: One is due to a current strip-sheet, of finite width 2X, lying in the x-y plane (between -X and +X in figure 2b), infinitely long in the y-direction, consisting of a constant current/length K. The other is the bifilar circuit due to two infinitely long parallel wires, at $x=\pm X$, carrying constant current I. Thus, end effects are neglected, which may be reasonable for most points along a long, narrow array with a slow variation of currents with y.

## MAGNETIC FIELD

These assumptions allow us to approximate the magnetic field at any point as due to current sources which are constant in the y-direction and extend to positive and negative infinity in the y-direction. Thus, they produce a magnetic field independent of y. The sheet current affects only the y-component of the field, while the wire currents affect only the x and z components. Hence, we may superimpose the two independent magnetic field systems, expressed in c.g.s. units, as follows:

$$B_x = 2\mu I z \left[\frac{1}{(x+X)^2 + z^2} - \frac{1}{(x-X)^2 + z^2}\right] \quad (1)$$

$$B_z = 2\mu I \left[\frac{x-X}{(x-X)^2 + z^2} - \frac{x+X}{(x+X)^2 + z^2}\right] \quad (2)$$

$$B_y = 2\mu K \left[\arctan\left(\frac{x-X}{z}\right) - \arctan\left(\frac{x+X}{z}\right)\right] \quad (3)$$

where $B_x$ and $B_z$ are produced by the wire currents and $B_y$ is produced by the strip-sheet current; $\mu$ is the magnetic permeability. This field distribution is illustrated in figure 3. Note that the magnetic field due to the wire current inhibits particle motion in the y-direction, while the magnetic field due to the sheet current inhibits particle motion in the x-z plane. These expressions may be used to estimate magnetic intensities. The magnetic field intensity on the surface of the panel due to the wires is given by equation (2) evaluated at z=0, namely,

$$B_z = -\frac{4\mu I}{X} \cdot \frac{1}{1-(x/X)^2} = -0.4 \text{ gauss} \cdot \frac{1}{1-(x/X)^2} \quad (4)$$

for I = 100 kiloamp and X = 1 km

The magnetic field intensity on the surface of the panel due to the sheet current is given by equation (3) evaluated at z=0, namely,

$$B_y = -2\pi\mu K = -0.0314 \text{ gauss} \quad (5)$$

for $K = 10^5$ amp/20 km = 5 amp/meter

Thus, the field due to the wires is an order of magnitude stronger than the field due to the sheet current, over most of the length of the panel.

## CONSERVATION OF CANONICAL MOMENTUM. DYNAMICAL LIMITS OF THE MOTION

Using equations (1)-(3) and some manipulation, the equations of motion, neglecting electric forces, can be written

$$\ddot{x} = -\frac{2e\mu K}{m}\psi\dot{z} - \frac{1}{2}\frac{\partial}{\partial x}\dot{y}^2 \quad (6)$$

$$\ddot{z} = +\frac{2e\mu K}{m}\psi\dot{x} - \frac{1}{2}\frac{\partial}{\partial z}\dot{y}^2 \quad (7)$$

$$\dot{y} = \frac{e\mu I}{m}(\phi - \phi_0) + \dot{y}_0 \quad (8)$$

where

$$\psi \equiv \arctan\left(\frac{x+X}{z}\right) - \arctan\left(\frac{x-X}{z}\right) \tag{9}$$

$$\phi \equiv \ln\left[\frac{(x-X)^2 + z^2}{(x+X)^2 + z^2}\right] \tag{10}$$

and the subscripts "o" denote initial conditions. The quantities m and e denote the particle mass and charge, respectively. We have an integral of the motion in y, and $\dot{y}^2/2$ represents an effective potential function of x and z, whose gradient represents an effective electric field. From conservation of energy we have

$$\dot{x}^2 + \dot{y}^2 + \dot{z}^2 = v^2 = \text{constant} \tag{11}$$

so that

$$\dot{x}^2 + \dot{z}^2 = v^2 - \dot{y}^2 = v^2 - \left(\dot{y}_o + \frac{e\mu I}{m}(\phi - \phi_o)\right)^2 \geq 0 \tag{12}$$

The region in x-z space where equation (12) is satisfied represents a region of physically allowed motion; the rest of x-z space is dynamically forbidden. A dynamical analysis along similar lines was applied to current collection by a charged satellite in the LEO geomagnetic field by Parker and Murphy in reference 2. Clearly, $\phi$ is constant on a circle whose center is on the x-axis.

From analysis of equations (10) and (12) it can be shown that an electron or ion with a given energy may reach a point x on the surface with angles of incidence such that (for positive x)

$$-1 \leq \dot{y}/(\dot{x}^2 + \dot{y}^2 + \dot{z}^2)^{1/2} \leq 1 - P/Q \tag{13}$$

where

$$P \equiv \ln\left[\frac{(x+X)^2}{(x-X)^2}\right] \tag{14}$$

(X is the position of the wire)

and

$$Q \equiv \frac{p(E)}{e\mu I} \quad \left(= 1445\frac{\sqrt{E(ev)}}{I(amp)} \text{ for protons; } = 33.7\,\frac{\sqrt{E(ev)}}{I(amp)}\sqrt{1+E(mev)} \text{ for electrons}\right) \tag{15}$$

where p(E) denotes the particle momentum as a function of energy E. The quantity Q is the ratio of particle momentum to the "magnetic" scale momentum $e\mu I$. p(E) is $\sqrt{2mE}$ for nonrelativistic particles. The additional square-root factor for electrons is [illegible] lativistic correction.

Note that

(a) particles of all energies coming from infinity can reach x=0 (the mid-line of the panel), and

(b) particles coming from infinity with energy E cannot hit beyond $x=x_{max}$

where

$$\frac{x_{max}}{X} = \tanh\left(\frac{Q}{2}\right) \tag{16}$$

(The latter derives from the condition that P/Q in equation (13) cannot exceed 2.) Thus, no particles with finite energy can hit the wire.

The magnetic scale of momentum, eμI, is $1.6 \times 10^{-16}$ gm-cm/sec when I is 100 kiloamp. (It is proportionally lower as I decreases along the array.) Electrons with this momentum (Q=1) are relativistic, with energy E=2.5 mev. In geosynchronous orbit we may assume that the ions are protons. They would have the magnetic scale of momentum if their energy were E=4.8 kev. In low-earth orbit, assuming oxygen ions, the corresponding energy is 300 ev. This implies a simple criterion based on the magnitude of Q. If Q is small, the particles cannot penetrate. Assuming that the particle temperatures in geosynchronous orbit may at times be 1 ev ("cold" particles) and at other times be 10 kev ("hot" particles), we infer that electrons of both temperatures, whose values of Q are $3.37 \times 10^{-4}$ and $3.37 \times 10^{-2}$, respectively, are easily excluded from most of the array surface. Similarly, the cold protons, with Q=0.0144, are also excluded. The 10-kev protons, however, with Q=1.445, may penetrate to the surface. In low-earth orbit, where the particle temperatures are of the order of 0.1 ev, both ions and electrons are easily excluded. The above Q-values are obtained assuming I=100 kiloamp, i.e., they are appropriate for the high-current end of the array. It should be noted that Q is related to the gyro-radius $R_g$, evaluated at the mid-line of the array, based on the magnitude of $B_z$ from equation (4); namely, the gyronumber $R_g/X$ is equal to Q/4.

## FLUXES

The dynamical limits represented by equations (13)-(15) may be used to compute particle fluxes at the surface. For a monoenergetic isotropic particle velocity distribution, the number of particles hitting unit area on the surface in unit time, at a distance x from the center-line, may be shown to be given by

$$F_{mono}(E) = \frac{n_o}{4}\sqrt{\frac{2E}{m}}\left\{1 - \frac{1}{\pi}\cos^{-1}A + \frac{A}{\pi}\sqrt{1 - A^2}\right\} \tag{17}$$

where A = 1 - P/Q,

$n_0$ is the particle number density at infinity, E and m are the particle energy and mass, and P and Q are given by equations (14) and (15). Thus, the factor in brackets becomes unity as P/Q becomes small. It vanishes if P/Q exceeds 2 (see equation (16)). If Q is small, P must also remain small, which means that surface impacts are confined to the vicinity of the center-line (x=0). Also, the flux distribution is symmetric about the center-line.

The flux due to a Maxwellian velocity distribution may be computed by integrating equation (17) over the energy distribution. This must be done numerically, by quadratures. Using Parker's quadrature method (ref. 3), dimensionless flux-profile data were computed, for electrons and protons, for temperatures T=10 kev and T=1 ev, typical values in geosynchronous orbit. The profiles (positive x only), are shown in tables 1-3, for y-values along the panel from 20 km down to zero, in steps of 2 km. The current I is assumed to be proportionally reduced as y decreases. The x-values range from zero to 1 km in steps of 0.1 km. The second column, labelled "$x_{max}$", shows how close to the wire (at x=1) particles of energy equal to the temperature can get (equation (16)).

Table 1 shows 10-kev proton profiles. The profiles are fairly well spread out over the surface, but with a sharp dropoff to zero at x=1 km, as expected. As y decreases the coverage of the surface becomes greater as the wire current decreases. The data of the table indicates that the proton gyroradius $R_g$ at E=10 kev and B=0.4 gauss (midway between the currents at y=20 km - see equation (4)) is 2.3 km, a size comparable with the width of the array. $E_{scale}$=4.8 kev is the magnetic scale energy, and the thermal energy 10 kev is larger than this. Hence there is consistency between the lack of shielding of 10-kev ions and the sizes of $E_{scale}$ and $R_g$. Note that the density is unity (ambient value) along the axis (x=0), and along the last row, for y=0 (where the current and magnetic field vanish). Recalling that these results represent dynamical limits, it is evident that the "ridge" of unit density along the axis (middle of panel) should actually be significantly lower due to the inhibition of motion in the x-z plane by the sheet-current magnetic field.

Table 2 shows 1-ev proton profiles. Here, there is essentially no coverage of the surface (except very near x=0. See the $x_{max}$ column). Hence the shielding is very effective. This is also consistent with the thermal energy of 1 ev being much less than $E_{scale}$=4.6 kev, as well as with $R_g$=23 m at 0.4 gauss being much less than 1 km.

Table 3 shows 10-kev electron profiles. Here, the penetration is slightly greater, particularly near y=0. However, the panel may be considered effectively shielded. Calculations were also done for 1-ev electrons, but results are not shown here, since, as may be expected, the penetration is completely negligible, much less than in table 3. For the 10-kev and 1-ev electrons, $R_g$ has the values 53 meters and 53 cm, respectively.

These numerical-integration results are consistent with expectations based on the simple criterion of Q compared with unity, where E is set equal to kT.

## POSSIBLE INCREASE OF SOLAR CELL LIFETIME

It is estimated that 80 percent of the radiation damage to solar cells would be due to the trapped Van Allen belt electrons with energies up to 5 mev (E. G. Stassinopoulos, private communication, 1978), against which magnetic shielding is possible. (The remaining 20 percent is due mostly to cosmic rays which are not presently shieldable.) From the simple criterion of this paper that Q be less than unity, we see from equation (15) that electrons up to several mev in energy are prevented from reaching a large fraction of the array surface in the vicinity of the 100-kiloamp currents. In particular, from equations (15) and (16), with E=5 mev and I(y) represented by 5000y amp, with y in km, the area shielded against up-to-5-mev electrons lies between x(km)=tanh [0.923x20/y(km)] and x(km)=1.0. At y=20 km, this range of positions is from 730 m to 1000 m. Hence the range of protected positions is 270 m, within which the solar cell lifetime would be prolonged by a possible factor of 5.

We would like to thank James G. Laframboise for his helpful comments.

## REFERENCES

1. Rockwell International Report, Satellite Power System (SPS) Feasibility Study, SD76-SA-0239-2, 1976.

2. Parker, L. W.; and Murphy, B. L.: Potential Buildup on an Electron-Emitting Ionospheric Satellite. J. Geophys. Res., vol. 72, 1967, p. 1631.

3. Parker, L. W.: Calculation of Sheath and Wake Structure about a Pillbox-Shaped Spacecraft in a Flowing Plasma. Proceedings of the Spacecraft Charging Technology Conference, C. P. Pike and R. R. Lovell, Eds., Report AFGL-TR-77-0051/NASA TMX-73537, Feb. 1977, p. 331.

Table 1.

DYNAMICAL LIMITS
MAGNETICALLY SHIELDED FLUX PROFILES
10 kev IONS

2 km x 20 km
100000 amps
$E_{scale}$ = 4.8 kev
$R_g$ = 2.3 km*

| y(km) | $x_{max}$ | x(km) → 0. | .1 | .2 | .3 | .4 | .5 | .6 | .7 | .8 | .9 | 1.0 |
|---|---|---|---|---|---|---|---|---|---|---|---|---|
| 20 | .62 | 1.00 | .92 | .80 | .66 | .51 | .36 | .23 | .12 | .04 | .00 | 0. |
| 18 | .67 | 1.00 | .94 | .83 | .70 | .56 | .42 | .29 | .17 | .07 | .01 | 0. |
| 16 | .72 | 1.00 | .95 | .85 | .74 | .62 | .49 | .35 | .23 | .11 | .03 | 0. |
| 14 | .77 | 1.00 | .95 | .88 | .78 | .67 | .56 | .43 | .30 | .17 | .06 | 0. |
| 12 | .83 | 1.00 | .96 | .90 | .82 | .73 | .63 | .51 | .39 | .25 | .11 | 0. |
| 10 | .89 | 1.00 | .97 | .92 | .86 | .79 | .70 | .61 | .49 | .36 | .20 | 0. |
| 8 | .95 | 1.00 | .98 | .94 | .90 | .84 | .78 | .70 | .61 | .49 | .32 | 0. |
| 6 | .98 | 1.00 | .99 | .96 | .93 | .89 | .85 | .79 | .72 | .63 | .48 | 0. |
| 4 | 1.00† | 1.00 | .99 | .98 | .96 | .94 | .91 | .88 | .84 | .78 | .68 | 0. |
| 2 | 1.00† | 1.00 | 1.00 | .99 | .99 | .98 | .97 | .96 | .94 | .91 | .87 | 0. |
| 0 | 1.00 | 1.00 | 1.00 | 1.00 | 1.00 | 1.00 | 1.00 | 1.00 | 1.00 | 1.00 | 1.00 | 0. |

*Ion gyroradius based on B = 0.4 gauss midway between wire currents at 100000 amp. Note: $R_g$ is larger than array width of 2 km.

†Very close to but less than unity.

Table 2.

DYNAMICAL LIMITS
MAGNETICALLY SHIELDED FLUX PROFILES
1 ev IONS

2 km x 20 km
100000 amps
$E_{scale}$ = 4.8 kev
$R_g$ = 23 m*

| | | x(km) → | | | | | | | | | | |
|---|---|---|---|---|---|---|---|---|---|---|---|---|
| y(km) | $x_{max}$ | 0. | .1 | .2 | .3 | .4 | .5 | .6 | .7 | .8 | .9 | 1.0 |
| 20 | .01 | 1.00 | 0. | 0. | 0. | 0. | 0. | 0. | 0. | 0. | 0. | 0. |
| 18 | .01 | 1.00 | 0. | 0. | 0. | 0. | 0. | 0. | 0. | 0. | 0. | 0. |
| 16 | .01 | 1.00 | 0. | 0. | 0. | 0. | 0. | 0. | 0. | 0. | 0. | 0. |
| 14 | .01 | 1.00 | 0. | 0. | 0. | 0. | 0. | 0. | 0. | 0. | 0. | 0. |
| 12 | .01 | 1.00 | 0. | 0. | 0. | 0. | 0. | 0. | 0. | 0. | 0. | 0. |
| 10 | .01 | 1.00 | 0. | 0. | 0. | 0. | 0. | 0. | 0. | 0. | 0. | 0. |
| 8 | .02 | 1.00 | 0. | 0. | 0. | 0. | 0. | 0. | 0. | 0. | 0. | 0. |
| 6 | .02 | 1.00 | 0. | 0. | 0. | 0. | 0. | 0. | 0. | 0. | 0. | 0. |
| 4 | .04 | 1.00 | 0. | 0. | 0. | 0. | 0. | 0. | 0. | 0. | 0. | 0. |
| 2 | .07 | 1.00 | .07 | 0. | 0. | 0. | 0. | 0. | 0. | 0. | 0. | 0. |
| 0 | 1.00 | 1.00 | 1.00 | 1.00 | 1.00 | 1.00 | 1.00 | 1.00 | 1.00 | 1.00 | 1.00 | 0. |

*Ion gyroradius based on B = 0.4 gauss midway between wire currents at 100000 amp. Note: $R_g$ is small compared with array width of 2 km.

Table 3.

DYNAMICAL LIMITS
MAGNETICALLY SHIELDED FLUX PROFILES
10 kev ELECTRONS

2 km x 20 km
100000 amps
$E_{scale}$ = 2.5 mev
$R_g$ = 53 m*

| | | x(km) → | | | | | | | | | | |
|---|---|---|---|---|---|---|---|---|---|---|---|---|
| y(km) | $x_{max}$ | 0. | .1 | .2 | .3 | .4 | .5 | .6 | .7 | .8 | .9 | 1.0 |
| 20 | .02 | 1.00 | 0. | 0. | 0. | 0. | 0. | 0. | 0. | 0. | 0. | 0. |
| 18 | .02 | 1.00 | 0. | 0. | 0. | 0. | 0. | 0. | 0. | 0. | 0. | 0. |
| 16 | .02 | 1.00 | 0. | 0. | 0. | 0. | 0. | 0. | 0. | 0. | 0. | 0. |
| 14 | .02 | 1.00 | 0. | 0. | 0. | 0. | 0. | 0. | 0. | 0. | 0. | 0. |
| 12 | .03 | 1.00 | 0. | 0. | 0. | 0. | 0. | 0. | 0. | 0. | 0. | 0. |
| 10 | .03 | 1.00 | 0. | 0. | 0. | 0. | 0. | 0. | 0. | 0. | 0. | 0. |
| 8 | .04 | 1.00 | .00 | 0. | 0. | 0. | 0. | 0. | 0. | 0. | 0. | 0. |
| 6 | .06 | 1.00 | .02 | 0. | 0. | 0. | 0. | 0. | 0. | 0. | 0. | 0. |
| 4 | .08 | 1.00 | .12 | .00 | 0. | 0. | 0. | 0. | 0. | 0. | 0. | 0. |
| 2 | .17 | 1.00 | .50 | .12 | .01 | .00 | 0. | 0. | 0. | 0. | 0. | 0. |
| 0 | 1.00 | 1.00 | 1.00 | 1.00 | 1.00 | 1.00 | 1.00 | 1.00 | 1.00 | 1.00 | 1.00 | 1.00 |

*Electron gyroradius based on B = 0.4 gauss midway between wire currents at 100000 amp. Note: $R_g$ is small compared with array width of 2 km.

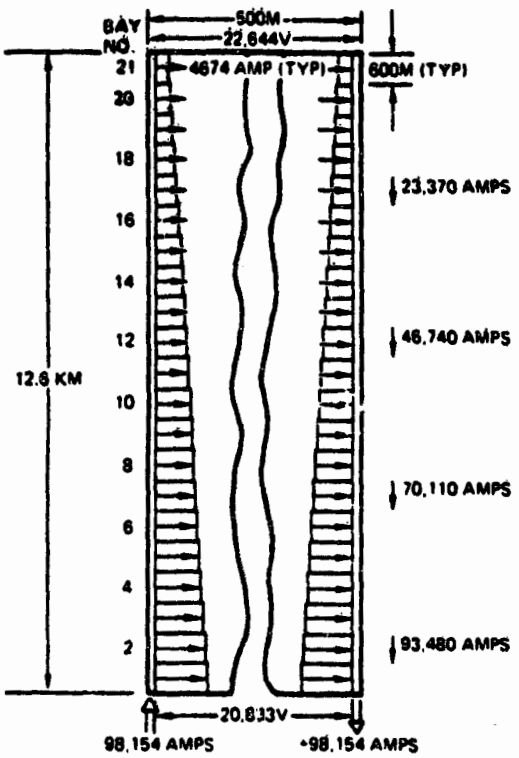


Figure 1. - Sample design configuration (Rockwell).

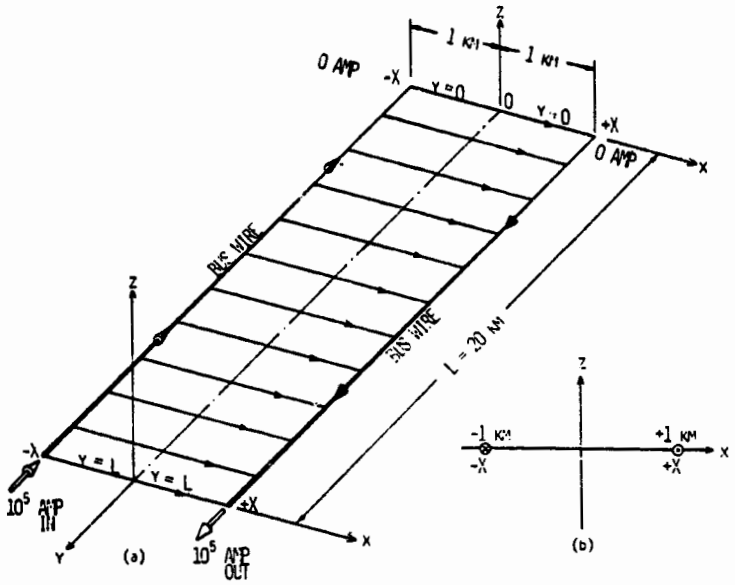


Figure 2. - Current distributions in solar array panel analytical model.

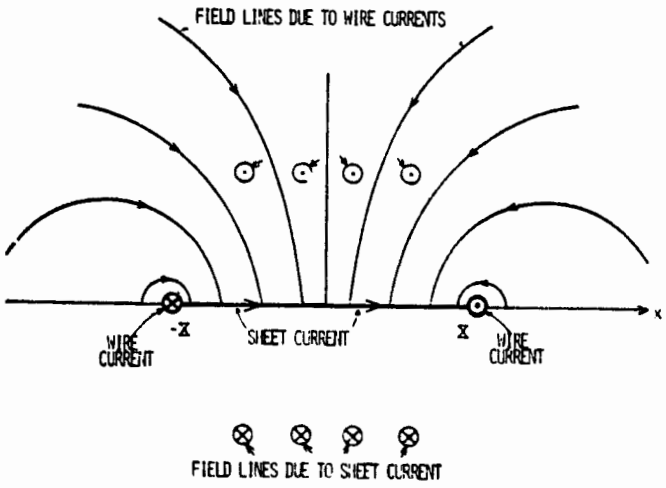


Figure 3. - Magnetic field systems in solar array panel analytical model.